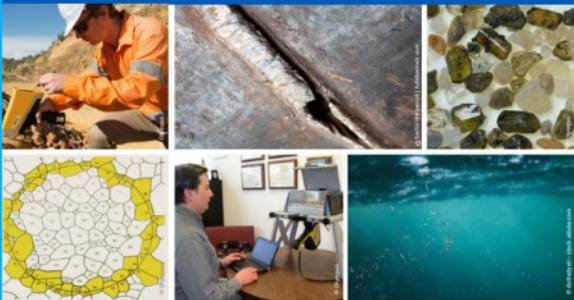




# 2<sup>nd</sup> Advanced Optical Metrology Compendium

## Advanced Optical Metrology

Geoscience | Corrosion | Particles | Additive Manufacturing: Metallurgy, Cut Analysis & Porosity



**EVIDENT**  
**OLYMPUS**

**WILEY**

The latest eBook from **Advanced Optical Metrology**.  
Download for free.


This compendium includes a collection of optical metrology papers, a repository of teaching materials, and instructions on how to publish scientific achievements.

With the aim of improving communication between fundamental research and industrial applications in the field of optical metrology we have collected and organized existing information and made it more accessible and useful for researchers and practitioners.

**EVIDENT**  
**OLYMPUS**

**WILEY**

# The effect of bird droppings on the corrosion of steel and aluminum used in offshore applications

Fredrik Forr<sup>1</sup> | Erlind Mysliu<sup>1</sup> | Jan Halvor Nordlien<sup>1,2</sup> | Andreas Erbe<sup>1</sup> 

<sup>1</sup>Department of Materials Science and Engineering, NTNU, Norwegian University of Science and Technology, Trondheim, Norway

<sup>2</sup>Innovation & Technology - Precision Tubing, Hydro Extrusions, Håvik, Norway

## Correspondence

Andreas Erbe, Department of Materials Science and Engineering, NTNU, Norwegian University of Science and Technology, 7291 Trondheim, Norway.  
Email: [birddroppings@the-passivists.org](mailto:birddroppings@the-passivists.org)

## Abstract

Engineering materials in service are frequently exposed to bird droppings (BDs). In this study, the interaction has been studied of BDs from chicken with a carbon steel, AISI 316, 22% Cr duplex stainless steel (DSS), 25% Cr super duplex stainless steel (SDSS), carbon steel with a thermally sprayed aluminum (TSA) coating, and aluminum alloy EN AW 6082. Samples with and without BDs are exposed to a cyclic salt spray test for up to 692 h (29 days). Electrochemical experiments in the presence of BDs were conducted in a syringe-based droplet cell. Characterization of the corrosion products by infrared (IR) and Raman spectroscopy shows no build-in of organic components into the corrosion products in the samples exposed to BDs. In general, BDs affect the anodic dissolution mechanism of metals and increase the critical pitting potential. For carbon steel, a component of the BDs acts as an anodic inhibitor, leading to passivation of the surface and decreasing corrosion rates by 1–2 orders of magnitude. For 316, BDs increase the critical pitting potential but may facilitate crevice-like initiation of localized corrosion. There are negligible effects of BDs on the corrosion of SDSS, and no evidence either for adverse effects on DSS. TSA shows an increased corrosion rate by half to one order of magnitude with BDs, but its ability to galvanically protect a steel base material is not compromised. AW 6082 shows decreased corrosion rate, no difference in mass loss, but increased pitting in the presence of BDs. Overall, these model experiments may only be seen as the start of a more systematic understanding of the interaction of BDs with engineering materials.

## KEYWORDS

aluminium, bird excrements, bird faeces, bird-induced corrosion, electrochemical droplet cell, metallic coatings, stainless steel, steel, vibrational spectroscopy, weight loss

This is an open access article under the terms of the Creative Commons Attribution License, which permits use, distribution and reproduction in any medium, provided the original work is properly cited.

© 2022 The Authors. *Materials and Corrosion* published by Wiley-VCH GmbH.

## 1 | INTRODUCTION

Engineering materials in service are frequently exposed to bird droppings (BDs). Studies exist, for example, of the interaction of BDs with car paint,<sup>[1–3]</sup> copper and bronze which are frequently encountered in cultural heritage objects,<sup>[4–6]</sup> and highway structures consisting mainly of concrete.<sup>[7]</sup> The clear coat of car paint is degraded by the BDs through enzymatic hydrolysis.<sup>[1–3]</sup> Copper and bronze suffered from significant chemical damage,<sup>[4,5]</sup> producing corrosion products not expected for atmospheric corrosion.<sup>[4]</sup> Traces of deposits originating from birds were found in the patina on copper roofs.<sup>[8]</sup> No effect on the degradation of bronze was found from chloride-containing uric acid in model experiments,<sup>[6]</sup> whereas another study concluded there is damage of metals by uric acid.<sup>[9]</sup> Observation of increased roughness led to the conclusion that BDs degrade concrete and stone.<sup>[7,10]</sup> Stones used, for example, in historic churches are also broken down by the BDs.<sup>[11,12]</sup> Hence, BDs can compromise the lifetime of several materials.

The reported composition of BDs shows differences between different studies. Uric acid, proteins, ammonia, and nitrite have been shown to make up about 20% of the seabird-dropping composition.<sup>[13]</sup> BDs of urban pigeons proved to contain chemical elements not found in pigeons held at farms, without full quantitative analysis,<sup>[7]</sup> concluding that the diet plays a role in BD composition.<sup>[14,15]</sup> The number of soluble salts in BDs from urban pigeons was found to be 4%, where the anions present are sulfate, chloride, phosphate, fluoride, bromide, and nitrate, ranging from highest concentration to lowest.<sup>[12]</sup> The term “guano” is used to describe dried and solidified excrement, also in combination with several species, for example, bird- and bat guano.<sup>[16]</sup> Fresh bat excrement has a pH of 5.1–7.3.<sup>[17]</sup> However, when the excrement dries and solidifies, as shown for bat guano, the pH drops to 2.7–4.1.<sup>[17]</sup> How the effect is on BDs is not known, but others have assumed similar behavior.<sup>[18]</sup> Bacterial respiration occurring in the BDs can produce products that lower the pH of the droppings additionally.<sup>[16]</sup>

A current trend in the offshore industries is the creation of unmanned or normally unmanned installations, which most likely introduces a greater presence of birds on the installations.<sup>[18]</sup> In this study, the interaction of BDs with metallic structural materials important for offshore applications is investigated; the investigated materials are carbon steel, stainless steel, and aluminum, along with a metallic coating on steel, and thermal sprayed aluminum (TSA). Based on NORSOK standard M-001,<sup>[19]</sup> which describes the materials selection of steels, carbon steel, and 316 stainless steel are typically

used for topside structures, piping, and vessels. Carbon steel is also recommended to be coated to mitigate corrosion. For applications with higher demand for corrosion resistance, duplex stainless steels are recommended. These applications could be piping and vessels with corrosive fluids. In addition, these may also be used in pumps, and valve internals. Aluminium EN AW 6082 is recommended for “structural sections and components” in the NORSOK standard M-121.<sup>[20]</sup> TSA is a metallic coating that is often used on steel because of its excellent corrosion protection properties. In the event of a coating breakdown, exposing a small area of the base steel, the steel will be cathodically protected by the aluminum.<sup>[21,22]</sup>

The purpose of this study was to investigate how BDs affect the corrosion behavior of materials as introduced above. Corrosion has been assessed by salt-spray testing where samples were exposed with and without BDs. Following this test, the samples were visually examined, and characterized by Fourier transform infrared (FTIR) and Raman spectroscopy to evaluate the presence of organic components on the metal surfaces. Mass loss of the various samples was determined after removal of corrosion products. Electrochemical experiments were conducted in a syringe-based electrochemical droplet cell containing BDs in direct contact with the materials; polarisation resistance, and cathodic and anodic polarisation curves were measured. The main focus of this study is a comparison of the respective experiment in the presence and in the absence of BDs, and not a comparison of the different materials with each other. Likewise, a detailed interpretation of the corrosion mechanisms of the plain materials—as interesting as that may be—shall not be the focus of this study.

## 2 | MATERIALS AND METHODS

The raw data used in this study are available at DataverseNO.<sup>[23]</sup>

### 2.1 | BDs

The BDs used were provided by chickens from a local owner and were stored in an air-tight container in a fridge. Feathers and straws were removed with the best effort before use. For both the salt spray test and the electrochemical experiments, the BDs were mixed with water to create a slurry. The amount of water used to create the slurry was not constant as the consistency of the BDs varied. The pH of slurries of BDs in artificial seawater up to 60 g/L was between 8 and 8.25.



## 2.2 | Materials

Commercial materials were used for this study, as typically used in the shipyards building offshore structures. Table 1 lists the standardized composition of the different materials used in this study. The TSA sprayed on carbon steel had a thickness of 200–300 with a 25  $\mu\text{m}$  silicone resin sealer. The wire used for the TSA used in the experiments was of the grade EN AW 1050A (>99.5% Al). The composition of the coating is assumed to be close to that of the wire. None of the materials had a special pretreatment; in particular, AW 6082 was not anodized, while it is frequently anodized in applications. Samples were used as received, without polishing or grinding to have a surface that corresponds to the surface in-service conditions.<sup>[24]</sup>

## 2.3 | Salt spray test

Three samples of each material, in total of 18 samples, were prepared for a salt spray test. The samples were cut into  $4 \times 8\text{cm}^2$  rectangular pieces. These pieces were then rinsed with distilled water, acetone, and ethanol. All samples were then weighed individually before clear nail polish was applied on the edges of the samples to avoid edge effects (The backside of the sample was not protected, which leads to a different situation than in an application scenario). A BD slurry was spread on half the sample surface; this design was preferred over a design where twice as many samples with the full area exposed to BDs are used because the latter does not include effects from the practically important contact between a BD-containing side and a BD free side. Then the samples were placed in an Ascott CC450IP cyclic chamber. Because of the sample thickness, the standard sample holders could not be utilized. To ensure that water would run off, and not accumulate on the surface, the samples were

supported by a plastic piece. This gave the samples an angle of  $23^\circ$  to the horizontal plane. Images of the samples before testing and at different stages of the test are shown in Supporting Information: Section 1.

The testing was inspired by the ASTM G85-19 standard,<sup>[25]</sup> which is a cyclic test made to simulate rain, high humidity, and sunny weather. Cycle steps were 45 min spraying, 2 h dry air purge, and 3:15 h soaking at high relative humidity, all at  $49^\circ\text{C}$ .

A salt solution was made according to section 6.3 in the G85 standard (five parts NaCl dissolved in 95 parts drinking water). The initial pH of the solution was not adjusted to 2.8–3.0 as the standard suggests. The low pH would make the carbon steel corrode very fast, and therefore the initial pH was 6.5 for the salt solution. After 2 weeks of running (334 h), the most corrosion-resistant materials showed almost no corrosion. Thus, the solution pH was adjusted to 3.0 by concentrated acetic acid, as suggested by the G85 standard. Acidification was done to accelerate the corrosion process. The experiment proceeded under these conditions for an additional 358 h, resulting in a total exposure time of 692 h for the materials that were left in the chamber for the whole experiment. Supporting Information: Section 1 contains an overview of the time each sample was held in the salt spray chamber; the time was decided after a visual inspection of the samples at the given opening times. After 692 h the experiment was concluded and the remaining samples were removed from the chamber. When samples were removed from the chamber, they were rinsed in water to remove salt deposits and left to dry before storing them in individual plastic bags, following the ASTM G85-19 standard.

## 2.4 | Raman and FTIR spectroscopy

Both the areas exposed to BDs and areas without BDs exposed longest in the salt spray chamber were subjected

**TABLE 1** Composition of materials used here; except for thermally sprayed aluminum (TSA), these are standard values

Steel	Cr	Ni	C	Mn	Si	P	S	Mo	Fe	PREN
Carbon steel	–	–	0.4	–	–	–	–	–	Balance	–
AISI 316	16–18	10–14	0.08	2.0	1.0	0.045	0.030	2–3	Balance	25
22% Cr DSS	21–23	4.5–6.5	0.03	2.0	1.0	0.030	0.020	2.5–3.5	Balance	33
25% Cr SDSS	24–26	6–8	0.03	1.0	1.0	0.030	0.010	3–4	Balance	40
Aluminium	Mn	Fe	Mg	Si	Cu	Zn	Ti	Cr	Al	
EN AW 6082	0.40–1.00	0.5	0.60–1.20	0.70–1.30	0.10	0.20	0.10	0.025	Balance	
EN AW 1050A (TSA)	0.05	0.40	0.05	0.25	0.05	0.07	0.05	–	>99.5	

Note: Values are given as wt% and single values are maximum values. Abbreviations: DSS, duplex stainless steel; PREN, pitting resistance equivalent number; SDSS, super duplex stainless steel.

to post-mortem FTIR and Raman spectroscopic analysis. After removal from the salt spray chamber, samples were rinsed with water to remove soluble deposits and subsequently dried. No other cleaning step was conducted before measurements; in particular, the nail polish covering the edges and the corrosion products were only removed after spectroscopic experiments. The instruments used were Bruker Vertex 80v vacuum FTIR spectrometer and WITech Alpha 300R confocal Raman microscope.

The Raman spectra were recorded using a  $50\times$  magnification and a working distance of 9.1 mm. The laser (532 nm) was set to a power of  $(0.15 \pm 0.05)$  mW. The accumulation time was at least 60 s, with 6–10 accumulations.

In FTIR, samples were analyzed at grazing incidence. The light-exposed area was  $1.78\text{ cm}^2$ . The spectral resolution was set to  $4\text{ cm}^{-1}$ , with an accumulation of 100 scans for each measurement. Absorbance  $A$  was calculated in two different variants. First, a gold mirror was used as background to make corrosion product peaks visible against a noncorroding reference; the absorbance against this background is calculated as  $A = -\log_{10}(I_{\text{sample}}/I_{\text{gold}})$ , where  $I$  is the intensity of light recorded in the presence of the species indicated in the subscript. Second, spectra in which the corrosion products with BDs were used as samples against a reference of the side without BDs are also displayed to easily visualize the differences between the two surfaces. To that end, difference absorbance was calculated as  $A = -\log_{10}(I_{\text{BD}}/I_{\text{plain}})$ .

## 2.5 | Mass loss

After the spectroscopic analysis, the samples were weighed again to analyze the mass loss during exposure in the salt-spray chamber. For comparison of the corrosion rates between the side with and without BDs, the samples needed to be cut. They were cut across the middle of the sample, creating samples close to  $4 \times 4\text{ cm}^2$ , yielding an area exposed to BDs and an area without. These pieces were then weighed before and after the removal of the corrosion products. The corrosion products were removed chemically according to the ASTM G01 standard.<sup>[26]</sup> Supporting Information: Section 5 lists the details. Using this procedure, the backside of the samples where the front side is covered with BDs also contributes to the mass loss; it is difficult to fully quantitatively account for this effect, as the front sides were exposed directly to the salt spray to a large extent by the design of the chamber.

## 2.6 | Method of electrochemical experiments

A syringe was modified to fit a reference electrode and a platinum wire counter electrode through the rubber gasket of the syringe, based on a design published in the literature,<sup>[27]</sup> which in turn is based on previous scanning droplet cell designs.<sup>[28,29]</sup> The reference electrode was an Ag/AgCl/KCl (sat.); all electrode potentials in this study are reported with respect to this reference. The platinum wire was turned around the reference electrode. Approximately 115 mm of platinum wire with a diameter of 0.5 mm was submerged in the electrolyte. With an average area of  $0.2\text{ mm}^2$  for the working electrode (WE), this yields a CE to WE area ratio of 900. The shell of the syringe was then filled with a modified synthetic seawater electrolyte, based on ASTM standard D1141,<sup>[30]</sup> but without some of the minor components. The solution contained 24.53 g/L NaCl, 5.2 g/L  $\text{MgCl}_2$ , 4.09 g/L  $\text{Na}_2\text{SO}_4$ , 1.16 g/L  $\text{CaCl}_2$ , and 0.695 g/L KCl. All used salts had a purity of at least 98%. The pH was adjusted from 0.1 M NaOH to 8.9.

The upper part of the syringe, consisting of a gasket, reference electrode, and counter electrode, was then inserted into the shell to create a seal, as shown in Figure 1. While more sophisticated versions of movable, localized electrochemical cells exist that permit localized measurements,<sup>[31–34]</sup> the nature of the BDs made such an easy-to-handle set-up desirable. This setup allows the tip of the syringe to be filled with BDs to perform measurements on the metal when covered by BDs. The BDs must have the right consistency which is adjusted using distilled water; distilled water was used as there is

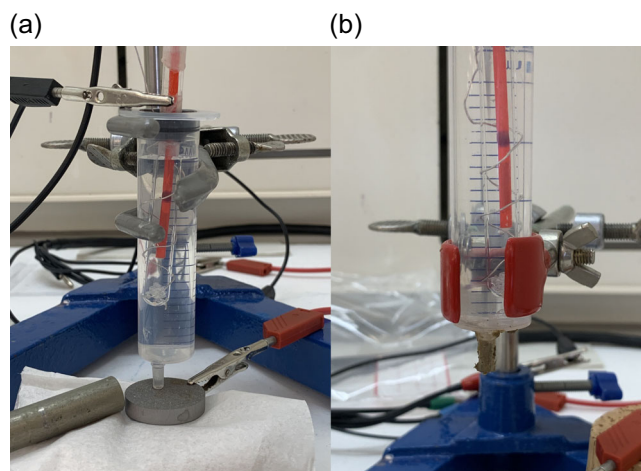


**FIGURE 1** (a) Setup used in electrochemical experiments, including an Ag/AgCl/KCl (sat.) reference electrode, platinum wire counter electrode, and electrolyte inside the syringe; (b) picture of the syringe with bird droppings (BDs) inside the syringe tip [Color figure can be viewed at [wileyonlinelibrary.com](http://wileyonlinelibrary.com)]

a certain salt content in the BDs of  $\approx 4\%$ . Too much water will lead to a flowing mass that will run out of the syringe; too little water results in the droppings plugging the syringe and contact loss during the experiment. The consistency of the BDs was varying, resulting in different amounts of water in the mixture. Overall, a cement-like consistency should be pursued. The setup was always installed inside a fume hood, regardless of whether the experiment was run with or without BDs. No other preparation of the BDs was performed.

The syringe setup was also tested with BDs deposited on top of the metal sample rather than inside the syringe. However, the BDs showed to act as a sponge in contact with the electrolyte and absorb a large amount of water, resulting in an exposed area that was both inconsistent and difficult to determine. There were also some challenges related to filling the tip of the syringe, caused by the consistency of the droppings.

## 2.7 | Procedure of electrochemical experiments

Metal samples were rinsed with ethanol, acetone, and distilled water before drying with pressurized air. The samples were not polished. The top of the syringe must be properly sealed so there is no leakage from the syringe. For the measurement including BDs, the BDs would be added to the syringe at this point by using a spatula. To avoid evaporation of the electrolyte during experiments, the syringe tip needed to be as close to the metal surface as possible without the risk of touching. The potentiostat used for the measurements was a Gamry 750 potentiostat.

Polarisation resistance, cathodic polarisation curves, and anodic polarisation curves were measured with this setup. Before any of these measurements were done, the open circuit potential (OCP) was measured for 15 min. The polarization resistance was measured by applying a potential of  $\pm 20$  mV around the OCP with a rate of 1.25 mV/s. The anodic polarisation curves were measured by increasing the potential with a rate of 2.5 mV/s from OCP until the potential was in the range of 1.0–1.3 V above the OCP, depending on the material to be measured. The cathodic curve was measured with the same parameters as the anodic curve but ended up at a potential of 1.0 V below the OCP. The sequence of the measurements could vary, but to ensure similar conditions, all measurements were made on an unused, clean, spot of the sample. Because all measurements were started at OCP, the terms OCP and corrosion potential  $E_{\text{corr}}$  are synonymous in this study. Differences in OCP between repeats should thus reflect the true variation

between experiments, for example, through heterogeneity of the materials surface.

## 3 | RESULTS

### 3.1 | Salt spray test

Images of the samples in the salt spray chamber after 49, 334, 592, and 692 h of exposure are shown in Supporting Information: Section 1. The first two samples, carbon steel and 316 were removed after 49 h. At this stage, the stainless steel samples showed only some small discoloring on their surfaces, while the TSA and AW 6082 did not show any discoloring. The carbon steel had discoloring on the whole surface visible in the picture.

After 334 h (14 days), some corrosion of the carbon steel was observed, indicated by the darker color around the edges and corrosion product on the sample holder. There was a slight increase in the discoloring for DSS sample 1. Salt deposits had accumulated around the edges of the TSA, along with some salt deposits on the 316.

Acidified solution led to high amounts of corrosion on the carbon steel, resulting in a short stint from 334 to 592 h. After 592 h (25 days), not much difference was observed in the condition for the carbon steel other than the darker color on the sample holder. 316 showed some more discoloring, both on the plain side and in the bottom right corner. AW 6082 had become more matt on the plain side, indicating some corrosion. The TSA had even more salt deposits on the surface.

After 692 h (29 days), TSA had more salt deposits on the surface, and AW 6082 showed some corrosion product on the side without BDs. The DSS and SDSS, however, showed almost no signs of corrosion, only minor discoloring on the surface. 316 showed more or less the same amount of discoloring as after 592 h.

Figure 2 shows pictures of the different samples after exposure; the BDs were on the right-hand side. For carbon steel, corrosion craters were visible on the side of the sample without BDs. The side with BDs had a more homogeneous topography. There was also a color difference between the two sides. For 316, there was a spotted pattern on the side with BDs. The left side showed a gradual increase in discoloring with increased exposure time. For DSS, the first and the last image showed more uniform corrosion on the side without BDs during exposure as well as a spotted pattern where BDs were present. Figure 2h showed less discoloring than the other two samples and no spotted pattern for the right side. For SDSS samples, there was very little corrosion visible for any exposure time. Most corrosion was visible



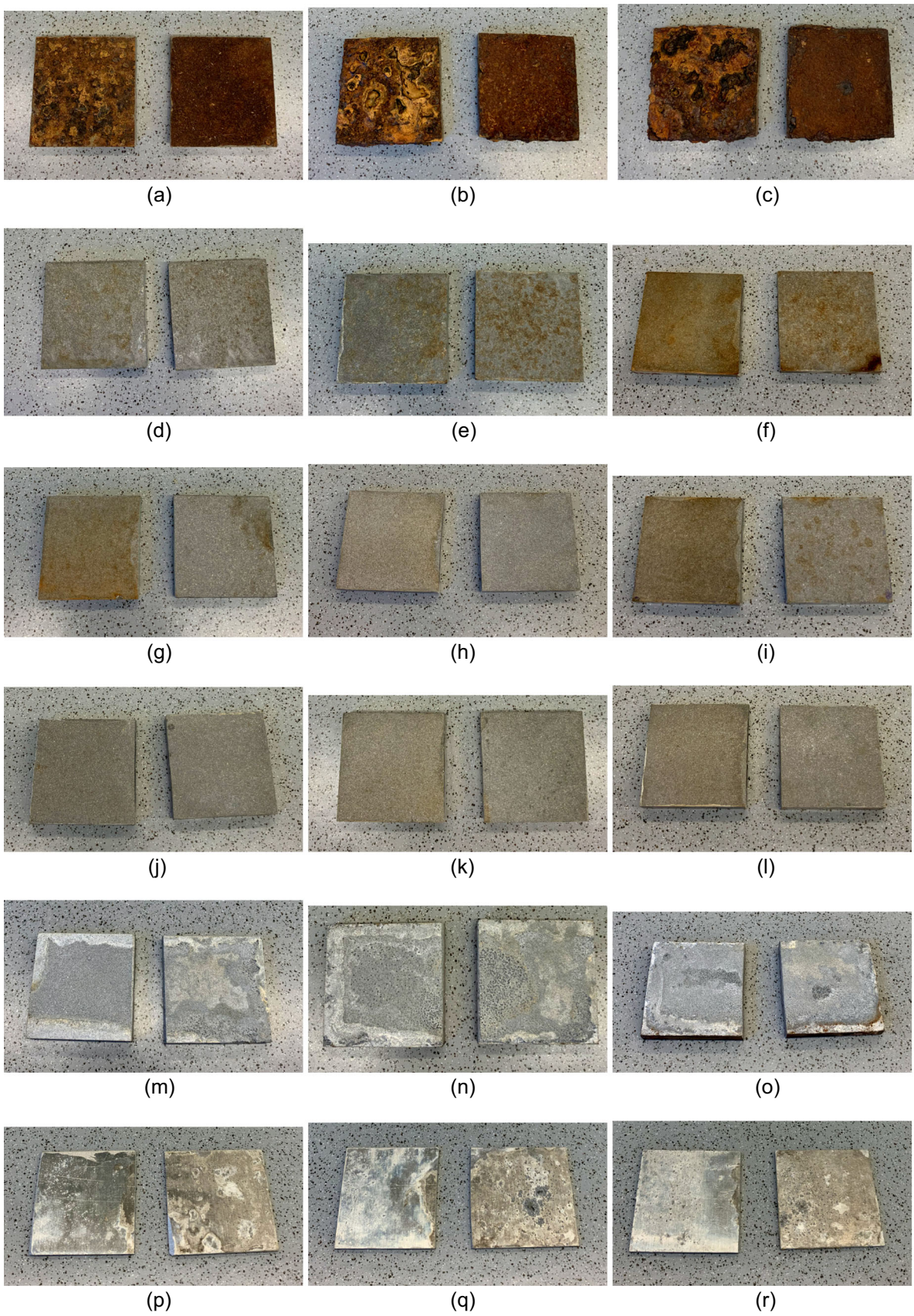


FIGURE 2 (See caption on next page)

on the plain side after 692 h. TSA samples showed a deposit around the edge of all samples. The first image (334 h) showed more corrosion on the side with BDs, later there was corrosion on both sides. For AW 6082 there was consistently at all times more pitting corrosion on the side with BDs; the differences increased with exposure time.

Sample masses before salt spray tests were converted into area density to be able to compare the samples before and after the salt spray test. The area density after removal of corrosion products is listed in Table 2. The raw data used to calculate the area density, and the data before removal of corrosion products are shown in Supporting Information: Section 5.

The area densities of the AW 6082 samples were nearly equal. For carbon steel, the presence of BDs decreased the rate of mass loss. For the three stainless steels, there was no clear trend of an effect of the BDs, but overall the mass loss was rather low. For TSA, the BDs increased slightly the rate of mass loss.

After salt spray testing, the samples have been characterized by FTIR spectroscopy (Supporting Information: Section 3) and by Raman spectroscopy (Supporting Information: Section 4). While this characterization yielded relevant data for understanding the corrosion process of the materials themselves, the spectra did not reveal characteristic consistent differences between the samples with and without BDs. Therefore, these spectra are not discussed in detail here; a summary is given in Supporting Information: Sections 3 and 4.

### 3.2 | Electrochemical experiments

An overview of the parameters derived from polarisation curves is shown in Table 3. The data from polarisation resistance measurements is shown in Supporting Information: Section 2.

Polarisation curves for carbon steel are shown in Figure 3. In the presence of BDs, a passive region occurred in the anodic polarisation curves, with a significant increase in current around 250 mV. This increase can be attributed to pitting. There was also an increase in polarisation resistance and  $E_{\text{corr}}$  in the presence of BDs. In a preliminary study to this one, polarisation curves were measured in a classical

electrochemical cell using dilute dispersions of BDs of up to 60 g/L in the same electrolyte. In these experiments, the corrosion current density  $i_{\text{corr}}$  increased up to concentrations of 45 g/L, however, dropped to the same value as in the absence of BDs for 60 g/L.

Polarisation curves for 316 stainless steel are presented in Figure 4. The critical pitting potential  $E_{\text{pit}}$  increased in the presence of BDs. The curves with BDs also showed little to no metastable pitting before  $E_{\text{pit}}$ . The polarization resistance was not that easy to comprehend, as there were no clear trends in the curves, but already a significant variation in the individual materials.

DSS proved to be a difficult material to work with, as there were a lot of fluctuations in the OCP. Consequently, many attempts were needed to get reproducible measurements. Figure 5 shows the polarisation curves with and without BDs. The DSS showed less metastable pitting when there were BDs present in the system. There was little difference in the OCP between the systems with and without BDs. The polarization resistance (Supporting Information: Section 2) without BDs had bigger deviations than the measurements where BDs were present. Qualitatively, the system with BDs was more stable as the OCP and curves were easier to reproduce. The observation of metastable pitting is also a possible explanation for the large fluctuations of the OCP.

Figure 6 shows the polarisation curves for SDSS; these curves show little differences in the  $E_{\text{corr}}$  range that was measured. SDSS is the material that shows the least change in the presence of BDs. There were more differences between the samples in the polarisation resistance measurements, both in terms of OCP and noise in the measurements.

The polarization curves for TSA are presented in Figure 7. There was an increase in the potential where the pitting initiates when BDs were present. The polarization resistance for the TSA was lower with BDs compared to the plain surface. There were some variations in the measurements.

AW 6082 also showed large variations of OCP, making it hard to find stable starting conditions. Stable polarisation curves obtained (Figure 8) showed a distinct difference in  $E_{\text{pit}}$ . With an increase of  $\approx 500$  mV, this is the biggest difference seen in any of the materials studied here. Because of the difficulties to find a stable OCP, the measurements of the polarisation resistance proved to be hard in the absence of BDs, which is why only two curves

**FIGURE 2** Samples after different exposure times in salt spray test; sample with bird droppings (BDs) on the right in the respective panel. Carbon steel after (a) 49 h, (b) 334 h, (c) 592 h; 316 after (d) 49 h, (e) 334 h, (f) 692 h; duplex stainless steel (DSS) after (g) 334 h, (h) 692 h, (i) 692 h (repeat); super duplex stainless steel (SDSS) samples after (j) 334 h, (k) 592 h, (l) 692 h; thermally sprayed aluminum (TSA) samples after (m) 334 h, (n) 592 h, (o) 692 h; AW 6082 after (p) 334 h, (q) 692 h, (r) 692 h (repeat). [Color figure can be viewed at [wileyonlinelibrary.com](https://onlinelibrary.wiley.com/doi/10.1002/maco.202213533)]



**TABLE 2** Area density of the samples ( $\rho_{A,0}$ , area density before experiments;  $\rho_{A,plain}$ , area density after removal of corrosion products of the side without bird droppings [BDs];  $\rho_{A,BD}$ , area density after removal of corrosion products for the side with BDs)

Material	Exp. time [h]	$\rho_{A,0}$ [g/cm <sup>2</sup> ]	$\rho_{A,plain}$ [g/cm <sup>2</sup> ]	$\rho_{A,BD}$ [g/cm <sup>2</sup> ]
Carbon steel	49	4.47	4.35	4.44
	334	4.42	4.16	4.20
	592	4.40	3.74	4.08
316	49	4.47	4.47	4.45
	334	4.48	4.44	4.46
	692	4.47	4.46	4.41
Duplex stainless steel (DSS)	334	4.63	4.59	4.59
	692	4.67	4.65	4.65
	692	4.61	4.60	4.57
Super duplex stainless steel (SDSS)	334	5.18	5.14	5.14
	592	5.23	5.18	5.21
	692	5.18	5.13	5.13
Thermally sprayed aluminum (TSA)	334	4.62	4.60	4.57
	592	4.64	4.62	4.57
	692	4.55	4.48	4.45
AW 6082	334	0.40	0.39	0.39
	692	0.39	0.39	0.40
	692	0.39	0.39	0.39

Note: Raw data and data before removal of corrosion products in Supporting Information: Section 5.

were obtained (Supporting Information: Section 2). The polarization resistance was much higher when BDs were present compared to the plain surface. Qualitatively, the OCP was more stable, for example, because of inhibition of metastable pitting, when BDs were present which makes it easier to get reproducible measurements.

From the polarization curves presented above, Tafel extrapolation was utilized to find  $i_{corr}$  and  $E_{corr}$ . Obtained parameters are summarised in Table 3. The polarisation resistance of most of the materials were fluctuating, and for some materials up to the order of several M $\Omega$ cm<sup>2</sup>. Large polarisation resistance is expected for passive materials. Also, the fact that there are several orders of magnitude difference for some materials between different measurements is not uncommon for passive materials, leading to large statistical uncertainty. These results are thus not discussed quantitatively.

## 4 | DISCUSSION

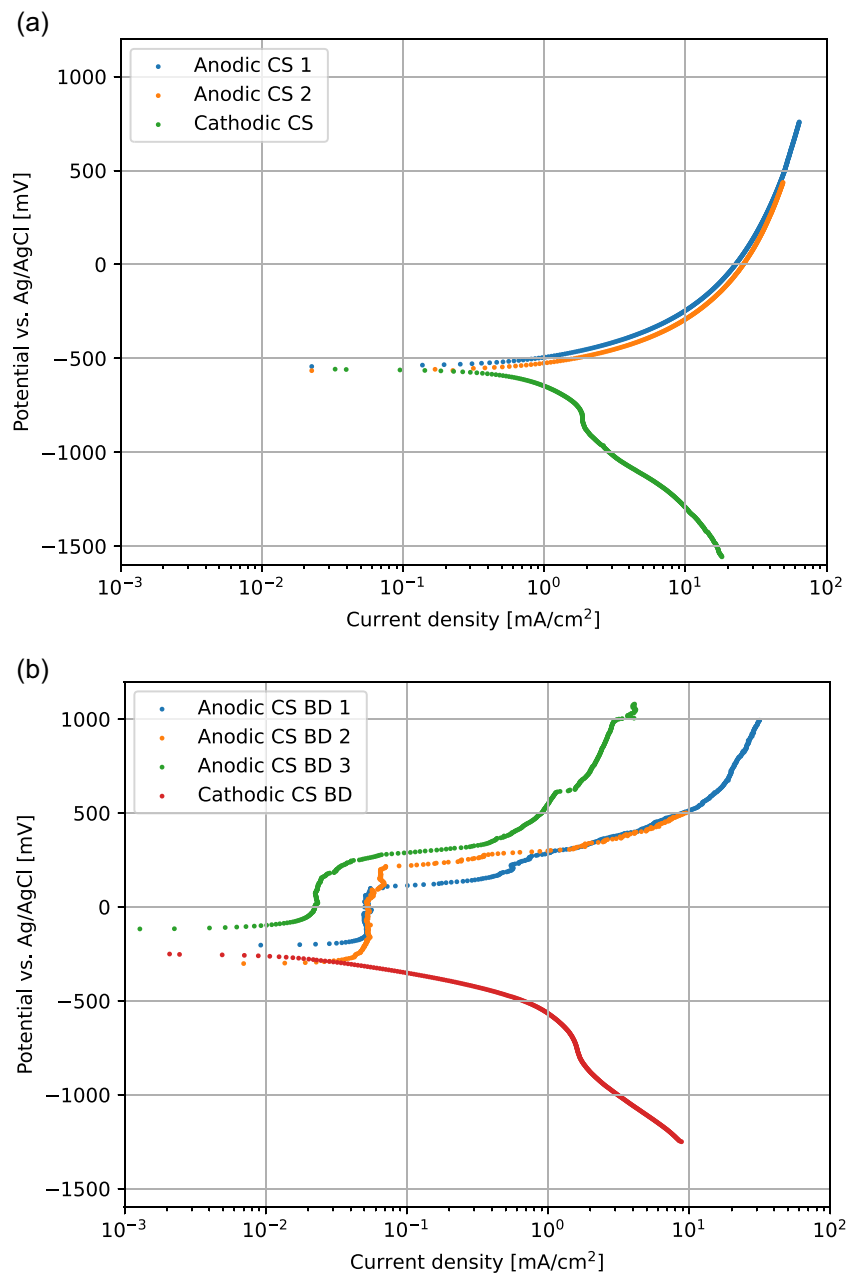
### 4.1 | General aspects

There is no evidence for the occurrence of new, different corrosion products under the influence of BDs, as evidenced by the absence of spectral features in the IR or Raman spectra which occur only in the areas covered by BDs. This absence of bird-specific corrosion products applies to all investigated materials. Consequently, no organic substances are to a significant extent built into the corrosion products that form. The absence of different corrosion products does, however, not rule out adsorption of compounds to the surface during and after corrosion processes, and an effect on the kinetics in situ. The fact that

**TABLE 3** Different quantities obtained from electrochemical experiments (CS, carbon steel; CR, corrosion rate from  $i_{corr}$ ;  $E_{corr}$ , corrosion potential from polarisation curves;  $E_{pit}$ , critical pitting potential [where clearly visible];  $i_{corr}$ , corrosion current density)

Material	Without bird droppings (BDs)				With BDs			
	$i_{corr}$ [mA/cm <sup>2</sup> ]	$E_{corr}$ [mV]	CR [mm/year]	$E_{pit}$ [mV]	$i_{corr}$ [mA/cm <sup>2</sup> ]	$E_{corr}$ [mV]	CR [mm/year]	$E_{pit}$ [mV]
CS	$(6.7 \pm 0.5) \cdot 10^{-1}$	$-580 \pm 28$	7.82	–	$(2.2 \pm 1.5) \cdot 10^{-2}$	$-233 \pm 76$	0.25	$150 \pm 50$
316	$(4.0 \pm 0.5) \cdot 10^{-2}$	$-255 \pm 10$	0.47	–50	$(7.3 \pm 3.2) \cdot 10^{-3}$	$-165 \pm 50$	0.085	350
Duplex stainless steel	$(1.1 \pm 0.4) \cdot 10^{-1}$	$-437 \pm 81$	1.28	–	$(7.3 \pm 0.4) \cdot 10^{-4}$	$-185 \pm 10$	0.085	–
Super duplex stainless steel	$(3.7 \pm 2.3) \cdot 10^{-4}$	$90 \pm 42$	0.0043	–	$(8.0 \pm 2.8) \cdot 10^{-4}$	$-155 \pm 36$	0.0093	–
Thermally sprayed aluminum	$(2.5 \pm 2.1) \cdot 10^{-6}$	$-800 \pm 283$	0.00003	–200	$(3.3 \pm 0.4) \cdot 10^{-5}$	$-656 \pm 50$	0.00036	$125 \pm 125$
AW 6082	$(2.0 \pm 1.4) \cdot 10^{-4}$	$-663 \pm 53$	0.0022	$-550 \pm 50$	$(1.0 \pm 0.1) \cdot 10^{-4}$	$-685 \pm 10$	0.0011	0

**FIGURE 3** Polarisation curves for carbon steel without (a) and with (b) bird droppings [Color figure can be viewed at [wileyonlinelibrary.com](http://wileyonlinelibrary.com)]



some Raman spectra show differences, for example, in fluorescence background and in inorganic corrosion products does not contradict this conclusion, because Raman spectra are measured highly localized, and the corrosion product distribution is in any case heterogeneous.

Electrochemical measurements are not adversely affected by the presence of the BDs on the surface. The porous, poorly defined BDs are expected to add an additional resistance in the electrolyte, which (a) would affect polarisation resistance measurements if it is too high, and (ii) currents in general by an Ohmic potential drop. The fact that for materials such as carbon steel with low polarisation resistance the measurement of appropriate curves is possible shows that the variation and differences

observed on the passive materials are indeed related to the materials' properties, and not to problems with the cell. There is an enrichment of dissolution products in the porous BDs, evidenced by the rather large differences in starting potential of the different polarisation curves with BDs, which are not present without BDs. Since all measurements are done on a new spot on the surface, the surface should be in the same condition. Typical variation between different regions of the surfaces should be accounted for in the measurements without BDs, but these differences are much smaller. The only possibility for aging of a component is thus the BDs in the syringes.  $E_{\text{CORR}}$  with BDs will therefore to a larger degree vary with time than potentials under free corrosion in free solution.

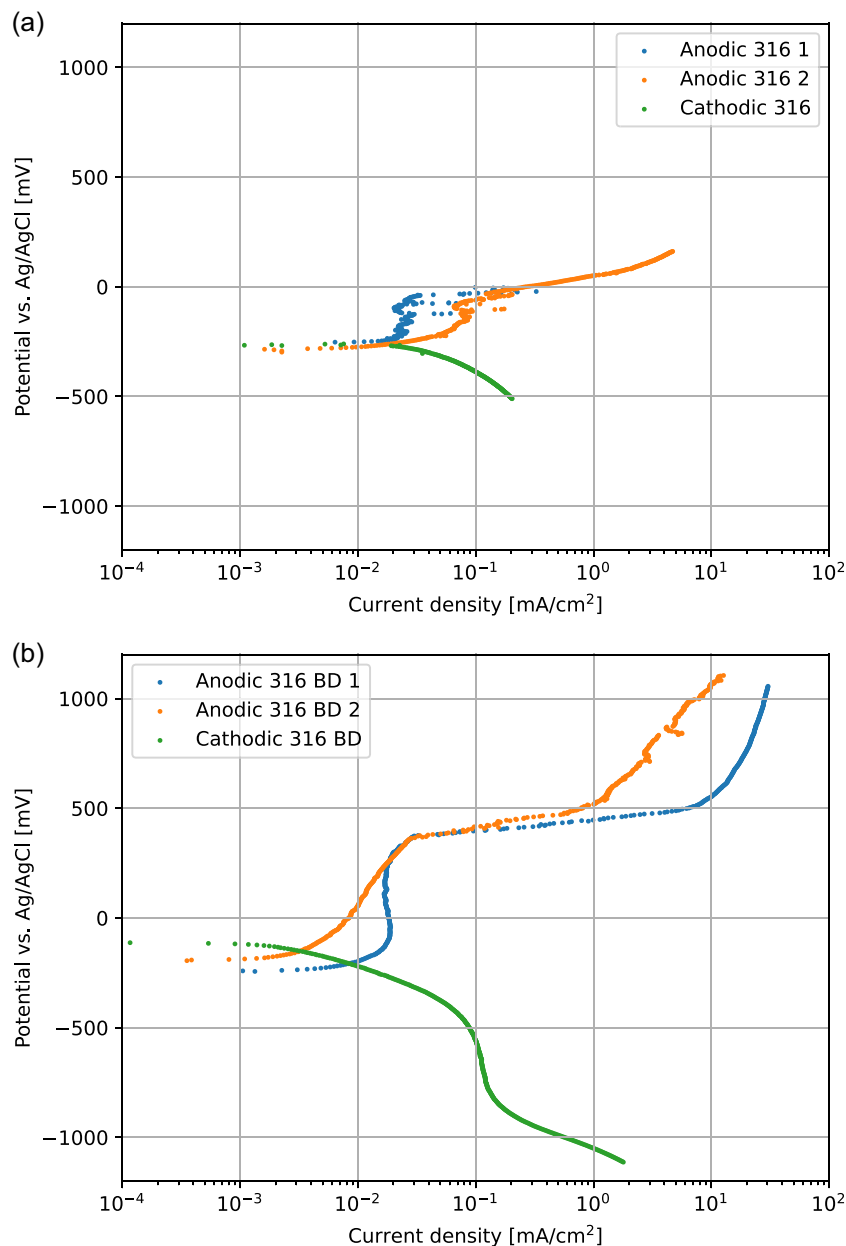


**FIGURE 4** Polarisation curves for 316 without (a) and with (b) bird droppings [Color figure can be viewed at [wileyonlinelibrary.com](http://wileyonlinelibrary.com)]

The electrochemical data has been interpreted based on the premise that the BDs themselves do not contribute significantly via redox-active compounds to the overall currents. The three orders of magnitude differences between corrosion currents detected on steel and TSA justify this assumption. In such slow polarisation curves, one would also expect only limited release and diffusion rates of species to the surface.

## 4.2 | Carbon steel

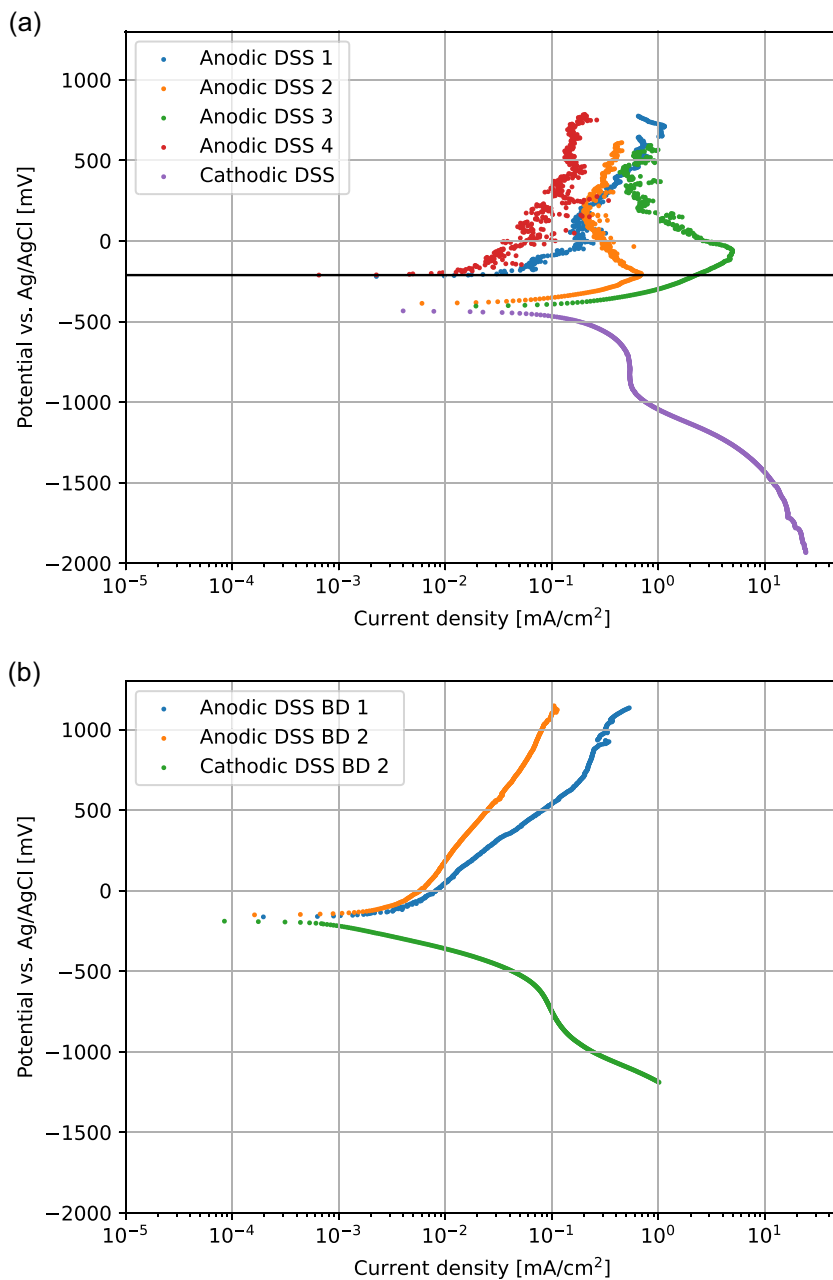
The BDs slow down the corrosion of carbon steel by adding an additional barrier and by passivating the surface, in line with decreased mass loss, more

homogeneous topography, the appearance of a passive region in the anodic polarisation curves in the presence of BDs, the increase of  $E_{\text{corr}}$  accompanied by a decrease by one order of magnitude in  $i_{\text{corr}}$  in the presence of BDs, and the increased polarisation resistance with BDs. Already after 49 h salt spray test, there are differences in appearance of the surfaces. After longer exposure times the plain side shows bigger craters and the BDs side appears more homogeneous.

The protective effect of BDs becomes more pronounced with decreasing pH, shown by the ca. 50% reduced mass loss in the period between 334 and 592 h of exposure when the solution was acidified. At the same time, the mass loss per hour for plain carbon steel is two orders of magnitude higher from 334 to 592 h than from



**FIGURE 5** Polarisation curves for duplex stainless steel without (a) and with (b) bird droppings. Line in (a) highlights the open circuit potential for experiments 1 and 2 [Color figure can be viewed at [wileyonlinelibrary.com](http://wileyonlinelibrary.com)]



0 to 334 h. With BDs, however, the mass loss per hour is in the same order of magnitude throughout the whole experiment. Thus, lower pH accelerated the corrosion on the plain side of the sample, but not on the side with BDs. The BDs' pH when dry is believed to be somewhat similar to the solution at the end of the experiment.<sup>[17]</sup> The BDs positive effects are therefore more beneficial than the detrimental effects of the low pH and anions in the dry BDs.

The anodic polarization curves show a passive region in the presence of BDs which is absent in the plain material. At higher potentials, the polarisation curves strongly resemble the curve of a system with pitting. There is no direct evidence, for example, from IR or

Raman for what causes the passivation. Possible reasons are (i) formation of a dense barrier oxide layer on the surface, for example, from an oxidizing compound, or (ii) adsorption, for example, on monolayer or few-layer level, of a component from the BD. In the case of adsorption, the surface structure is likely significantly different after removal from the solution, which requires thus sophisticated experiments to prove.<sup>[35–37]</sup> There is no hint here that an increase in pH would have happened, which could also explain the formation of a passive oxide. Such an increase is also not likely based on the literature of BDs.<sup>[17]</sup> Inhibition effects can also be caused by a rather intricate influence on the defect structure of the forming oxide.<sup>[38]</sup>

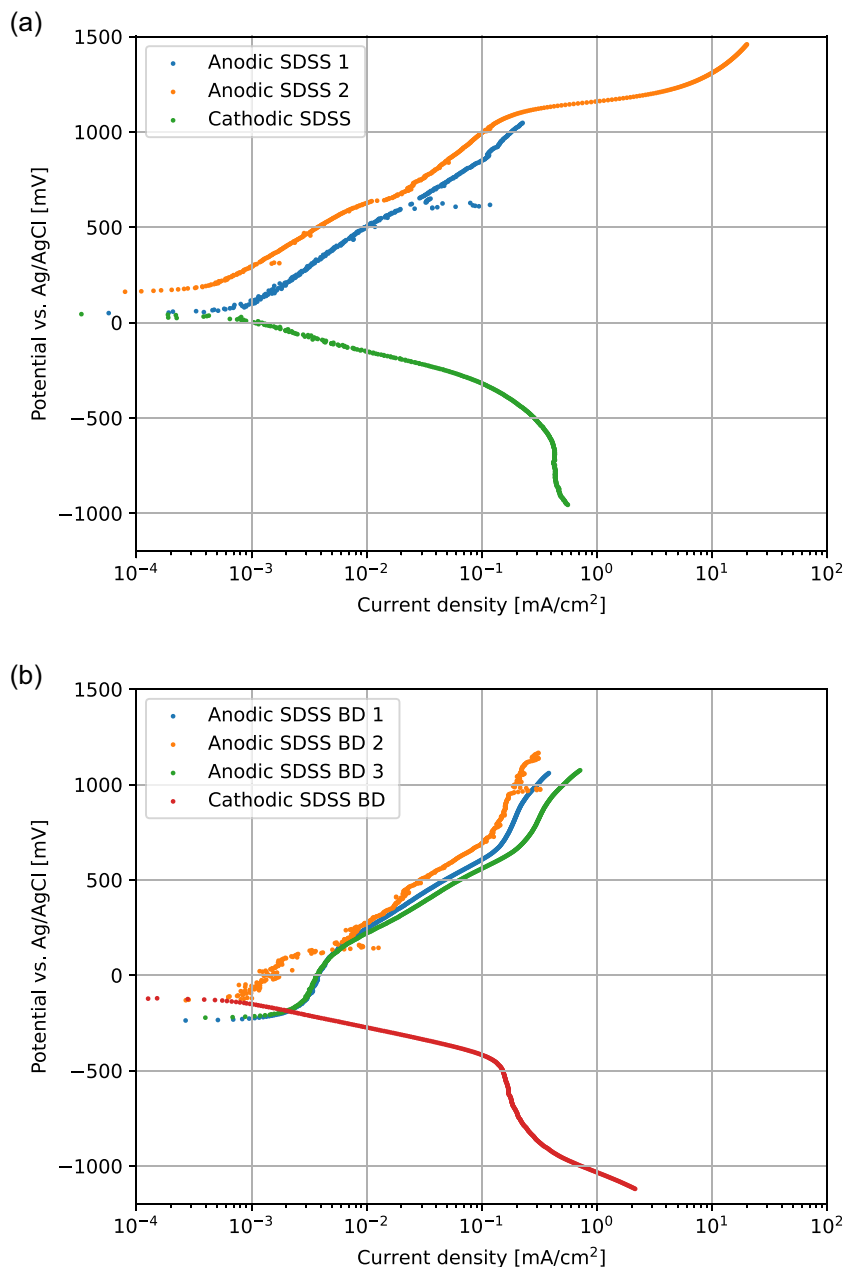


**FIGURE 6** Polarisation curves for super duplex stainless steel without (a) and with (b) bird droppings [Color figure can be viewed at [wileyonlinelibrary.com](https://onlinelibrary.wiley.com/doi/10.1002/maco.202213533)]

The cathodic processes are not affected by the BDs, as evidenced by the good agreement of the cathodic polarisation curves in the presence and absence of BDs. Therefore, the decreased corrosion rate must be caused by an effect on the anodic processes, which implies that a component from the BDs acts like an anodic corrosion inhibitor. This interpretation is in line with the decrease in  $i_{\text{corr}}$  above a certain BD concentration in dispersion as observed in preliminary experiments, as these often accelerate corrosion in low concentrations before they passivate materials.<sup>[39]</sup>

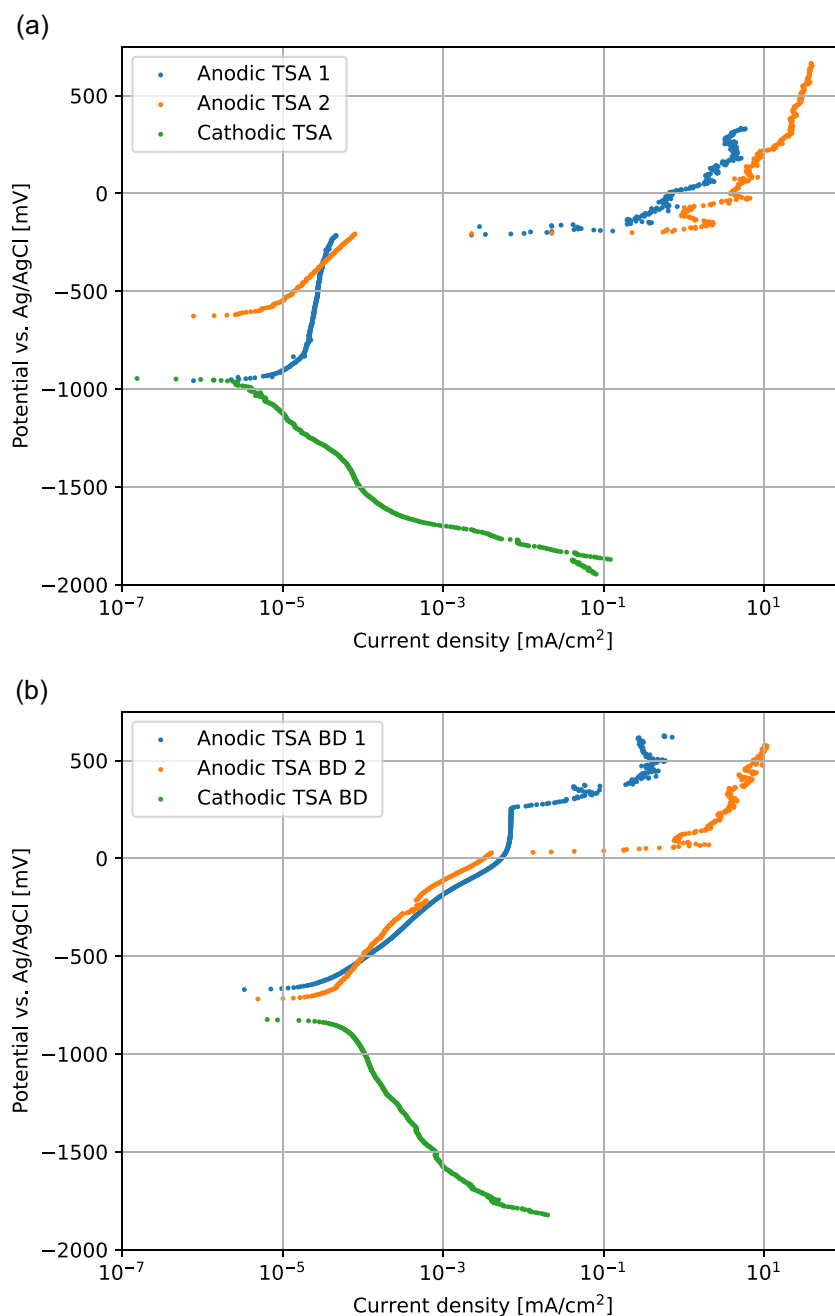
The passivation of the material in the presence of BDs could lead to localized corrosion, such as pitting. Indeed, an  $E_{\text{pit}}$  was observed in the anodic polarisation curves.

There were, however, no signs of pitting on the surface of the samples exposed to the salt-spray chamber. In applications, the galvanic coupling may shift the potential of a steel component to above  $E_{\text{pit}}$ , which must be avoided.

### 4.3 | 316

$E_{\text{pit}}$  of 316 is increased by nearly 500 mV in the presence of BDs. The 316 also shows less metastable pitting in the passive area in the presence of BDs. Up to  $E_{\text{pit}}$ , there is no difference in the dissolution kinetics between the system in the presence and absence of BDs. Thus, the BDs make

**FIGURE 7** Polarisation curves for thermally sprayed aluminum without (a) and with (b) bird droppings [Color figure can be viewed at [wileyonlinelibrary.com](http://wileyonlinelibrary.com)]



the 316 less prone to pitting initiation. A possible explanation of increased pitting resistance could be the decreased amount of anions near the surface due to poor ion transport through the BDs, or pH buffering effects near the surface.

The BDs do, however, initiate localized rust formation, possibly by crevice-like differential aeration effects. Visual inspection of the samples exposed for 334 and 692 h shows a spotted rust pattern on the surface with BDs, which is absent in the absence of BDs. As pit initiation is retarded by BDs (c.f. preceding paragraph), other, long-term effects must lead to this spotted, localized rust pattern observed. As the samples are

exposed in the salt spray tests over a much longer time and also during wet-dry cycles in the cyclic test compared to electrochemical experiments, we reason that the apparent contradiction between these two observations must be related to the barrier properties of the BDs and the consequent possibility for differential aeration in the inhomogeneously covered surface. This phenomenon requires a more detailed investigation.

There is no difference in uniform corrosion kinetics between the systems with and without BDs, even though this mode of corrosion is less relevant for this kind of material. Corrosion current densities agree well between the system with and without BDs, and the mass losses are



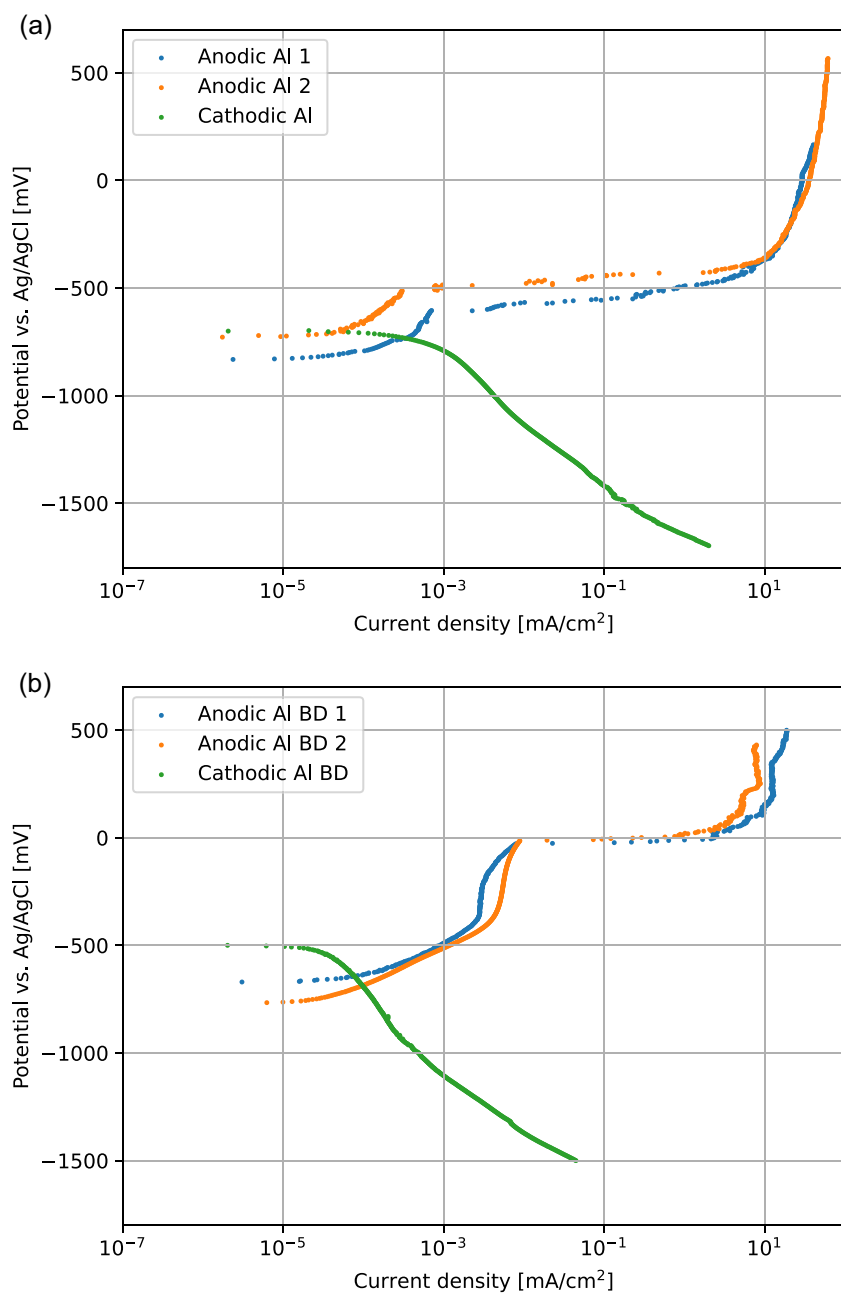


**FIGURE 8** Polarisation curves for AW 6082 without (a) and with (b) bird droppings [Color figure can be viewed at [wileyonlinelibrary.com](https://onlinelibrary.wiley.com/doi/10.1002/maco.202213533)]

relatively small in both cases. Before acidifying the test solution, the mass loss in the presence of BDs was slightly lower, and after acidifying slightly higher, than in their absence.

#### 4.4 | DSS

The stock from which the samples investigated here were taken may have suffered from a too heterogeneous surface quality, which manifests itself (i) in the large differences between two salt spray samples investigated for the same time and a rather nonintuitive trend with time without BDs (larger mass loss after 334 h of

exposure than for one sample after 692 h, large differences in appearance between two samples exposed for 692 h), (ii) large variations in  $E_{\text{CORR}}$  over several 100 s of mV, (iii) variations in the shapes of the anodic polarisation curves, and (iv) a higher uniform  $i_{\text{CORR}}$  than 316. The differences are not supposed to be caused by the presence of both the austenite and ferrite phases. The size of these phases is usually in the  $\mu\text{m}$  region, while the opening of the syringe is in the mm region. The area that is exposed to the electrolyte is therefore orders of magnitude larger than the austenitic and ferritic phases in the steel. Hence, the difference must be caused by differences in the chemical composition or microstructure of the steel across the samples. Alternatively,

a surface impurity that could not be removed by the comparably mild cleaning procedure may have been present. The peculiar features in the different repeats of the polarisation curves in the absence of BDs are not discussed here for this reason.

Similar crevice type of effects as discussed for 316 may also be observed here, with a rust spot appearing on one of the samples exposed for 692 h. However, here the effect is only observed for one sample and may thus be less common than for 316.

BDs do affect the electrochemical properties of DSS. The polarization curves with BDs display a different behavior than without. With BDs, the steel no longer shows a textbook-like passive domain in the polarisation curve, with potential independent current. There is a kink in the anodic branches of the polarisation curves around 300 mV which could indicate enhanced dissolution. This feature could originate from pitting initiated at an austenite/ferrite grain boundary which propagates slowly into the ferrite phase, as observed previously despite the fact that the ferrite phase is the phase richest in corrosion-resisting elements Cr and Mo.<sup>[40]</sup>

The presence of the BDs deactivates cathodic sites on the surface of DSS. There are clear differences in the cathodic polarisation curves comparing the system with and without BDs; the plateau typically attributed to the diffusion-limited oxygen reduction is almost one order of magnitude lower with BDs than without. This difference could be related to differences in the spontaneous convection patterns in the system,<sup>[41]</sup> however, as the current here is in between those observed for carbon steel and 316, it is more reasonable to attribute these differences to a different amount of cathodically active sites.

There is no evidence of a strong negative effect of the BDs in this system, however, for DSS this is not so easy to determine conclusively from the results obtained here. Again the rate of uniform corrosion, given by  $i_{\text{corr}}$ , decreases significantly (by two orders of magnitude) in the presence of BDs, though part of this decrease is because of the unreasonably high  $i_{\text{corr}}$  in the absence of BDs. Pit initiation may, however, be affected by the BDs adversely.

## 4.5 | SDSS

BDs have no significant effect on the corrosion resistance of SDSS. In the salt spray tests after 692 h, there is only very limited corrosion on both sides. Unlike 316 and one of the DSS samples, the SDSS does not show any spotted pattern on the side with BDs for any samples, that is, no evidence for localized rust formation. For all investigated

systems, SDSS also shows the least effect of BDs in the shape of the polarisation curves. While the mass loss was ca. 50% lower with BDs than without,  $i_{\text{corr}}$  was on the same order of magnitude but approximately twice as high with BDs; both changes, however, on an overall very low corrosion rate. Despite the  $\approx 250$  mV lower  $E_{\text{corr}}$  in the presence of BDs, SDSS is not significantly affected by BDs.

BDs do not affect the mechanism of metal dissolution or passivation in SDSS to a significant extent. The anodic branches with and without BDs have a similar shape. With BDs, there is a passive region when the potential is kept  $< \approx 100$  mV. At higher potential, slowly propagating pitting in the ferrite may occur up to 750 mV; the final increase above 1000 mV may be caused by pitting in both the austenite and ferrite phases,<sup>[42]</sup> or by the onset of oxygen evolution. Oxygen evolution is thermodynamically expected at so high potentials.

As for DSS, the BDs decrease the cathodic activity for oxygen reduction, as discussed in Section 4.4 most likely because of a decrease in the available amount of cathodic sites which are active for oxygen reduction.

## 4.6 | Thermally sprayed aluminum

The presence of BDs increases the self-corrosion rate of TSA, evidenced by 2–3 times increased mass loss in the early phase of salt spray exposure, much stronger prominence of corrosion products on the surface, and a one order of magnitude higher  $i_{\text{corr}}$  in the electrochemical experiments. The increase could be related to the ability of components in the BDs to complex  $\text{Al}^{3+}$ , increasing oxide solubility. Remarkably, the differences between salt spray samples were negligible in the second part of the exposure where the sample was acidic. The low pH in the second half of the experiments accelerated the corrosion of the plain TSA, without an additional effect from BDs. The higher mass loss may thus be explained by a decrease in pH during the drying cycles in the salt spray chamber; the low pH at high humidity may not represent a realistic use scenario, though. However, in the electrochemical experiments, the pH decrease is not expected to be so high. Therefore, a pH effect alone is not the only aspect. Likewise, both localized (judged by appearance) and uniform (judged by mass loss and  $i_{\text{corr}}$ ) corrosion rates increase. In the areas where BDs are present, these may act like a further organic coating, which is not desirable for TSA.<sup>[43]</sup>

The BDs do not compromise the ability of TSA to galvanically protect underlying steel, because its  $E_{\text{corr}}$  is unchanged by the presence of BDs and because of the large  $i_{\text{corr}}$ . For the samples exposed to the salt spray test

for the longest time, corrosion down to the substrate has been observed in some areas, with relatively little difference between the sample with and without BDs.

The BDs also change the anodic reaction mechanism for TSA, as evidenced by the differences in the anodic polarisation curves; whereas the current-potential relation in the absence of BDs is nearly potential independent in the passive region, there is a current increase in the presence of BDs. This behavior implies that the BDs compromise passivity in this system. On the other hand,  $E_{\text{pit}}$  increases when the BDs are present by 250-500 mV. Pitting itself is most likely not a big issue in a metallic coating that is supposed to protect the base material galvanically.

#### 4.7 | AW 6082

There is an increased susceptibility to pitting corrosion when exposed to acidic solution, even though the uniform corrosion rate in neutral or slightly alkaline solution decreases in the presence of BDs. Pits are clearly visible in the two samples with BDs exposed in the salt spray chamber for 692 h, however, only to a very limited extent in the sample exposed for 334 h; as the test solution was acidified after 334 h, this acidification in combination with the BDs is likely the reason for the observed pitting. Some pitting is also observed for the side without BDs. It must be noted that acidification in the accelerated tests may often be far from actual application conditions, as also noted for intergranular corrosion testing.<sup>[44]</sup> At the same time,  $i_{\text{corr}}$  decreases in the presence of BDs, and the mass loss is not detectable even in the samples exposed for 692 h. The latter finding is clear evidence for the absence of enhanced uniform corrosion in the presence of BDs. The BDs introduce an environment that may be harmful to non-anodized AW 6082.

The presence of BDs increases the passive region in the slightly alkaline chloride solution, shown by the polarisation curves. BDs thus increase  $E_{\text{pit}}$  by almost 500 mV; in general, in chloride solution, many aluminum alloys show  $E_{\text{pit}} \approx E_{\text{corr}}$ .<sup>[45]</sup> Thus, the trend that the BDs stabilize the oxide at least in the short term is not only true for steel, but also for aluminum. This phenomenon may therefore either relate to a specific chemical interaction that can take place in several metals and metal oxides or is a pH buffering effect from a component in the BDs. Note, however, that the passive current density is increased by the BDs by half an order of magnitude. This increase may indicate an interaction of a component in the BDs with the oxide, for example, with point defects, similar to what has been shown for zinc.<sup>[38]</sup>

The BDs also decrease the cathodic activity of cathodic inclusions, as shown by the lower cathodic currents. As opposed to the stainless steels above, the cathodic activity both of the diffusion-limited oxygen reduction and the hydrogen evolution may be decreased, though a full assignment of the different features in the curves is challenging.

## 5 | CONCLUSIONS

The corrosion behavior of different materials used in offshore applications has been investigated in the presence of BDs by salt spray tests and electrochemical experiments in a syringe-based droplet cell. In general, BDs affect the anodic dissolution mechanism, and decrease the rate of dissolution, except for the stainless steels they promote the passivity of materials, and where applicable also increase  $E_{\text{pit}}$ . At the same time, under acidic test conditions, BDs promote pitting initiation. At least for DSS, AW 6082, and possibly SDSS, they also reduce cathodic activity, possibly by blocking active sites for cathodic processes. Specifically, for the different materials, the following has been found.

- Carbon steel benefits from the presence of BDs with a lower corrosion rate, denser corrosion products, and passivation.
- 316 shows an increase in  $E_{\text{pit}}$  but at the same time a larger amount of rust spots in the salt spray tests in the presence of BDs.
- DSS showed conflicting results between different surface areas, but no evidence was found for a significant effect of BDs.
- SDSS shows a behavior that is nearly unaffected by the BDs.
- TSA suffers from localized corrosion and an increased self-corrosion rate under the BDs. While TSA is the material that is affected most by BDs, its function as a sacrificial coating is still maintained.
- AW 6082 suffers from localized corrosion underneath the BDs in acidic tests but also shows increased  $E_{\text{pit}}$  in near-neutral solution.

Overall, in practice, a lot will depend on details that could not be addressed in a study with a limited scope such as this. For instance, the diet of birds affects the composition of the BDs, and thus could have an effect on the corrosion rates and mechanisms. It remains an open question how far the experiments with chicken droppings conducted here can be transferred to other birds, and many mechanistic questions remain open for several of the investigated materials.



## AUTHOR CONTRIBUTIONS

Fredrik Forr was involved in the conceptualization, conducted all the investigations, and wrote the original draft. Erlind Mysliu developed the measurement methodology used for the electrochemical experiments and was involved in writing-review and editing. Jan Halvor Nordlien was involved in supervising, analysis, and writing-review and editing. Andreas Erbe was involved in conceptualization, analysis, project management, supervision, and writing-review and editing.

## ACKNOWLEDGMENTS

We thank Ørjan Ellingsen and Vegard Schøyen, Shell Norway, for bringing this topic to our attention and for providing sample material, Kurt Ekrem and Darko Petkovic, Randaberg Coating AS, for providing a TSA-coated sample, and Espen Strandheim, Aker Solutions ASA, for helpful discussions. Håvard Wilson, MainTech AS, is acknowledged for leading the industrial side of this project. For technical support, we thank Andrey Kosinskiy, Anita Storsve, and Marthe Folstad, for helpful discussions. Roald Lilletvedt and Iman Taji. Erlind Mysliu acknowledges a PhD scholarship in the frame of the project “Coated Recycled Aluminium - developing surfaces for well-adhering and corrosion resistant coating systems” supported by the Research Council of Norway (No. 309875), Hydro and Speira.

## CONFLICT OF INTEREST

The authors declare no conflict of interest.

## DATA AVAILABILITY STATEMENT

The data that support the findings of this study are openly available in NTNU Open Research Data (<https://dataverse.no/dataverse/ntnu>) at <https://doi.org/10.18710/VSZVHL>.

## ORCID

Andreas Erbe  <http://orcid.org/0000-0003-0225-2204>

## REFERENCES

- [1] H. Yari, M. Mohseni, B. Ramezanzadeh, *J. Coat. Technol. Res.* **2011**, *8*, 83.
- [2] H. Yari, M. Mohseni, B. Ramezanzadeh, N. Naderi, *Prog. Org. Coat.* **2009**, *66*, 281.
- [3] B. Ramezanzadeh, M. Mohseni, H. Yari, S. Sabbaghian, *Prog. Org. Coat.* **2009**, *66*, 149.
- [4] E. Bernardi, D. J. Bowden, P. Brimblecombe, H. Kenneally, L. Morselli, *Sci. Total Environ.* **2009**, *407*, 2383.
- [5] K. Balogh, Z. Slívz, K. Kreislóvá, *e-Monumentica* **2017**, *2017*, 5.
- [6] M. A. Ginez, A. Espinoza-Vázquez, F. J. Rodríguez-Gómez, *ECS Trans.* **2018**, *84*, 125.
- [7] C. P. Huang, G. Lavenburg, *Impacts of Bird Droppings and Deicing Salts on Highway Structures: Monitoring, Diagnosis, Prevention, Tech. Rep.* Delaware Center for Transportation, University of Delaware. <https://cpb-us-w2.wpmucdn.com/sites.udel.edu/dist/1/1139/files/2013/10/Rpt-221-Bird-Dropping-Impacts-Huang-DCTR422185-xk4gdv.pdf>
- [8] A. Stoch, J. Stoch, J. Gurbiel, M. Cichocińska, M. Mikołajczyk, M. Timler, *J. Mol. Struct.* **2001**, *596*, 201.
- [9] A. Vasiliu, D. Buruiana, *Int. J. Conserv. Sci.* **2010**, *1*, 83.
- [10] B. Cámara, M. Á. De Buergo, R. Fort, V. Souza-Egipsy, S. Perez-Ortega, A. De Los Ríos, J. Wierzchos, C. Ascaso, *Period. Mineral.* **2015**, *84*, 539.
- [11] P. Tiano, *Biodegradation of Cultural Heritage: Decay Mechanisms and Control Methods, Tech. Rep.* CNR - Centro di studio sulle "Cause Deperimento e Metodi Conservazione Opere d'Arte". [https://www.researchgate.net/publication/240635027\\_Biodegradation\\_of\\_Cultural\\_Heritage\\_Decay\\_Mechanisms\\_and\\_Control\\_Methods](https://www.researchgate.net/publication/240635027_Biodegradation_of_Cultural_Heritage_Decay_Mechanisms_and_Control_Methods)
- [12] M. Gómez-Heras, D. Benavente, M. Á. De Buergo, R. Fort, *Eur. J. Mineral.* **2004**, *16*, 505.
- [13] P. Szpak, J.-F. Millaire, C. D. White, F. J. Longstaffe, *J. Archaeol. Sci.* **2012**, *39*, 3721.
- [14] S. De La Peña-Lastra, *Sci. Total Environ.* **2021**, *754*, 142148.
- [15] D. H. R. Spennemann, M. J. Watson, *APT Bull. J. Preserv. Technol.* **2018**, *49*, 19.
- [16] R. Shahack-Gross, F. Berna, P. Karkanas, S. Weiner, *J. Archaeol. Sci.* **2004**, *31*, 1259.
- [17] C. M. Wurster, N. Munksgaard, C. Zwart, M. Bird, *Biogeochemistry* **2015**, *124*, 163.
- [18] S. Christensen-Dalsgaard, N. Dehnhard, B. Moe, G. H. R. Systad, A. Follstad. *Unmanned Installations and Birds. A Desktop Study on How to Minimize Area of Conflict, Nina Report.* Norwegian Institute for Nature Research. <http://hdl.handle.net/11250/2630793>
- [19] NORSOK Standard M-001. *Material Selection, Rev. 3, Tech. Rep.* Norwegian Technology Centre. <https://www.standard.no/pagefiles/1176/m-001.pdf>.
- [20] NORSOK Standard M-121. *Aluminium Structural Material, Tech. Rep.* Norwegian Technology Centre.
- [21] C. Holager, R. Johnsen, K. Nisancioglu, *NACE Int. Corros. Conf. Ser.* **2015**, 5570.
- [22] H. Wilson, R. Johnsen, C. T. Rodriguez, S. M. Hesjevik, *Mater. Corros.* **2019**, *70*, 293.
- [23] F. Oftedal Forr, E. Mysliu, J. H. Nordlien, A. Erbe, *Replication Data For: "The Effect of Bird Droppings on the Corrosion of Steels and Aluminium for Offshore Applications"*, NTNU Open Research Data, 10.18710/VSZVHL (2022).
- [24] A. J. Sendriks, *Corrosion of Stainless Steels*, 2nd ed., John Wiley & Sons, New York **1996**.
- [25] ASTM G85-19. *Standard Practice for Modified Salt Spray (Fog)testing, Tech. Rep.* ASTM International, West Conshohocken, 2019.
- [26] ASTM G1-03(2017)e1. *Standard Practice for Preparing, Cleaning, and Evaluating Corrosion Test Specimens, Tech. Rep.* ASTM International, West Conshohocken, 2017.
- [27] A. M. Panindre, K. H. Chang, T. Weirich, G. S. Frankel, *Corrosion* **2018**, *74*, 847.
- [28] A. W. Hassel, M. M. Lohrengel, *Electrochim. Acta* **1997**, *42*, 3327.

- [29] M. M. Lohrengel, A. Moehring, M. Pilaski, *Fresenius J. Anal. Chem.* **2000**, 367, 334.
- [30] ASTM D1141-98. *Standard Practice for the Preparation of Substitute Ocean Water*, Tech. Rep. ASTM International, West Conshohocken, 1998.
- [31] K. J. Jenewein, A. Kormányos, J. Knöppel, K. J. J. Mayrhofer, S. Cherevko, *ACS Meas. Sci. Au.* **2021**, 1, 74.
- [32] V. Shkirskiy, F. D. Speck, N. Kulyk, S. Cherevko, *J. Electrochem. Soc.* **2019**, 166, H866.
- [33] N. Jadhav, V. J. Gelling, *J. Electrochem. Soc.* **2019**, 166, C3461.
- [34] J. P. Kollender, A. I. Mardare, A. W. Hassel, *Electrochim. Acta* **2015**, 179, 32.
- [35] Y.-H. Chen, A. Erbe, *Corros. Sci.* **2018**, 145, 232.
- [36] A. Erbe, A. Sarfraz, C. Toparli, K. Schwenzfeier, F. Niu, *Soft matter at aqueous interfaces*, Vol. 917 of *Lect. Notes Phys.*, Springer, Cham, Switzerland **2016**, p. 459.
- [37] A. Erbe, S. Nayak, Y.-H. Chen, F. Niu, M. Pander, S. Tecklenburg, C. Toparli, *Encyclopedia of interfacial chemistry*, Elsevier, Oxford **2018**, p. 199.
- [38] A. Altin, M. Krzywiecki, A. Sarfraz, C. Toparli, C. Laska, P. Kerger, A. Zeradjanin, K. J. J. Mayrhofer, M. Rohwerder, A. Erbe, *Beilstein J. Nanotechnol.* **2018**, 9, 936.
- [39] I. Jevremović, Y.-H. Chen, A. Altin, A. Erbe, *Corrosion Inhibitors in the Oil and Gas Industry*, Wiley-VCH, Weinheim, Germany **2020**, pp. 359-382.
- [40] K. S. Siow, T. Y. Song, J. H. Qiu, *Anti-Corros. Methods Mater.* **2001**, 48, 31.
- [41] H. Wilson, A. Erbe, *Electrochem. Commun.* **2019**, 106, 106513.
- [42] H. Luo, X. G. Li, C. F. Dong, K. Xiao, *Arabian J. Chem.* **2017**, 10, S90.
- [43] O. Ø. Knudsen, A. Forsgren, *Corrosion Control Through Organic Coatings*, CRC Press, Boca Rayton, USA. **2017**.
- [44] S. Kumari, S. Wenner, J. C. Walmsley, O. Lunder, K. Nisancioglu, *J. Electrochem. Soc.* **2019**, 166, C3114.
- [45] D. Cicolin, M. Trueba, S. P. Trasatti, *Electrochim. Acta* **2014**, 124, 27.

## SUPPORTING INFORMATION

Additional supporting information can be found online in the Supporting Information section at the end of this article.

**How to cite this article:** F. Forr, E. Mysliu, J. H. Nordlien, A. Erbe, *Mater. Corros.* **2022**, 1–18.  
<https://doi.org/10.1002/maco.202213533>